

Published in final edited form as:

Science. 2005 May 27; 308(5726): 1318–1321. doi:10.1126/science.1108367.

Structural Bioinformatics-Based Design of Selective, Irreversible Kinase Inhibitors

Michael S. Cohen, Chao Zhang, Kevan M. Shokat, and Jack Taunton*

Program in Chemistry and Chemical Biology, and Department of Cellular and Molecular Pharmacology, University of California, San Francisco, CA 94143–2280, USA

Abstract

The active sites of 491 human protein kinase domains are highly conserved, which makes the design of selective inhibitors a formidable challenge. We used a structural bioinformatics approach to identify two selectivity filters, a threonine and a cysteine, at defined positions in the active site of p90 ribosomal protein S6 kinase (RSK). A fluoromethylketone inhibitor, designed to exploit both selectivity filters, potently and selectively inactivated RSK1 and RSK2 in mammalian cells. Kinases with only one selectivity filter were resistant to the inhibitor, yet they became sensitized after genetic introduction of the second selectivity filter. Thus, two amino acids that distinguish RSK from other protein kinases are sufficient to confer inhibitor sensitivity.

Phosphorylation of serine, threonine, and tyrosine residues is a primary mechanism for regulating protein function in eukaryotic cells. Protein kinases, the enzymes that catalyze these reactions, regulate essentially all cellular processes and have thus emerged as therapeutic targets for many human diseases (1). Small-molecule inhibitors of the Abelson tyrosine kinase (Abl) and the epidermal growth factor receptor (EGFR) have been developed into clinically useful anticancer drugs (2, 3). Selective inhibitors can also increase our understanding of the cellular and organismal roles of protein kinases. However, nearly all kinase inhibitors target the adenosine triphosphate (ATP) binding site, which is well conserved even among distantly related kinase domains. For this reason, rational design of inhibitors that selectively target even a subset of the 491 related human kinase domains continues to be a daunting challenge.

Structural and mutagenesis studies have revealed key determinants of kinase inhibitor selectivity, including a widely exploited selectivity filter in the ATP binding site known as the “gatekeeper.” A compact gatekeeper (such as threonine) allows bulky aromatic substituents, such as those found in the Src family kinase inhibitors, PP1 and PP2, to enter a deep hydrophobic pocket (4–6). In contrast, larger gatekeepers (methionine, leucine, isoleucine, or phenylalanine) restrict access to this pocket. A small gatekeeper provides only partial discrimination between kinase active sites, however, as ~20% of human kinases have a threonine at this position. Gleevec, a drug used to treat chronic myelogenous leukemia, exploits a threonine gatekeeper in the Abl kinase domain, yet it also potently inhibits the distantly related tyrosine kinase, c-KIT, as well as the platelet-derived growth factor receptor (PDGFR) (7).

We therefore sought a second selectivity filter that could be discerned from a primary sequence alignment. Among the 20 amino acids, cysteine has unique chemical reactivity and is commonly targeted by electrophilic inhibitors. In the case of cysteine protease inhibitors, the reactive cysteine is not a selectivity filter, because it is found in every cysteine protease

*To whom correspondence should be addressed. taunton@cmp.ucsf.edu.

and is essential for catalysis. Electrophilic, cysteine directed inhibitors of the EGFR kinase domain have also been reported (8), but here again, the cysteine does not act as a selectivity filter, because neither the electrophile nor the reactive cysteine is required for potent, selective inhibition by these compounds. In this report, we describe the rational design of selective kinase inhibitors that require the simultaneous presence of a threonine gatekeeper and a reactive cysteine, which are uniquely found in the C-terminal kinase domain of p90 ribosomal protein S6 kinases (RSKs).

We used a kinomewide sequence alignment (1, 9) to search for cysteines that, together with a threonine gatekeeper, could form a covalent bond with an inhibitor in the ATP pocket. We focused on the conserved glycine-rich loop, which interacts with the triphosphate of ATP and is one of the most flexible structural elements of the kinase domain (10). A cysteine near this solvent exposed loop is likely to have a lower pK_a and therefore to be more reactive than a cysteine buried in the hydrophobic pocket. Out of 491 related kinase domains in the human genome (1), we found 11 with a cysteine at the C-terminal end of the glycine-rich loop (Fig. 1A), a position usually occupied by valine. We next examined the gatekeeper in these kinases. Three closely related paralogs, RSK1, RSK2, and RSK4, have a threonine gatekeeper, whereas the remaining nine kinases, including RSK3, have larger gatekeepers (Fig. 1A). RSK1 and RSK2 are downstream effectors of the Ras-mitogen-activated protein kinase (MAPK) pathway and are directly activated by the MAPKs, ERK1 and ERK2 (11, 12). Mutations in the RSK2 gene cause Coffin-Lowry syndrome, a human disorder characterized by severe mental retardation (13). However, the precise roles of RSKs are poorly understood. All RSKs have two kinase domains. The regulatory C-terminal kinase domain (CTD) has the cysteine and threonine selectivity filters.

To exploit both selectivity filters in RSK family kinases, we needed a scaffold that could present an electrophile to the cysteine while occupying the hydrophobic pocket defined by the gatekeeper. Crystal structures of kinases with bound ATP analogs all reveal van der Waals contacts between a conserved valine, analogous to the cysteine we identified in RSKs (Fig. 1A), and the adenine C-8 position. We therefore designed and synthesized cmk and fmk (Fig. 1B), pyrrolopyrimidines that contained a chloromethylketone and a fluoromethylketone, respectively. The *p*-tolyl substituent was designed to occupy the putative hydrophobic pocket. Structurally related pyrazolopyrimidines interact similarly with Src family kinases (4–6). We hypothesized that the electrophilic halomethylketones would be within striking distance of the key cysteine in RSK1, RSK2, and RSK4 and that kinases with only one of the two selectivity filters would be resistant to the inhibitors.

We first tested the electrophilic pyrrolopyrimidines against the RSK2 CTD in vitro (14). Both fmk (Table 1) and cmk (15) inhibited RSK2 CTD activity with similar potencies, but we focused on fmk because of its greater chemical stability. To test whether both selectivity filters were required for fmk sensitivity, we expressed two CTD mutants, C436V, in which Cys⁴³⁶ was replaced with Val, and T493M, in which Thr⁴⁹³ was replaced with Met. Fmk was a potent and selective inhibitor of wild-type (WT) RSK2 [half-maximal inhibitory concentration (IC_{50}) = 15 nM], with greater than 600- and 200-fold selectivity over the C436V and T493M mutants, respectively (Table 1). To test whether fmk forms an irreversible covalent bond with RSK2, we prepared a biotinylated derivative (see Supporting Online Material). Biotin-fmk reacted irreversibly with WT RSK2, but not with the selectivity filter mutants, as shown by denaturing gel electrophoresis and Western blot analysis with streptavidin–horseradish peroxidase (HRP) (Fig. 2A). ERK2, required to activate RSK2 in vitro, was not labeled by biotin-fmk, despite the presence of a solvent-exposed cysteine in its ATP pocket (16).

We next tested the selectivity of biotin-fmk in a human epithelial cell lysate containing thousands of potentially reactive proteins. Biotin-fmk (1 μ M) reacted with only two proteins, and labeling was abolished by pretreatment with 1 μ M fmk (Fig. 2B). These ~90-kD proteins were shown to be RSK1 and RSK2 by quantitative immunodepletion with specific antibodies (Fig. 2C). A cell-permeable, fluorescent derivative of fmk was also found to be highly selective toward RSK1 and RSK2 when added to cells growing in culture (15).

The only known substrate of the RSK2 CTD is Ser³⁸⁶ of RSK2 itself (17, 18). Phosphorylation of Ser³⁸⁶ creates a docking site for phosphoinositide-dependent kinase 1 (PDK1), which then phosphorylates and activates the N-terminal kinase domain (NTD) (19). The activated NTD then phosphorylates downstream substrates. Treatment of serum-starved COS-7 cells with EGF induced Ser³⁸⁶ phosphorylation of endogenous RSK2, which was inhibited by fmk with a half-maximal effective concentration (EC₅₀) of ~200 nM (Fig. 3A). Thus, the CTD appears to be the primary kinase responsible for EGF-stimulated Ser³⁸⁶ phosphorylation, consistent with results obtained with kinase-inactive mutants (17, 18). Fmk (10 μ M) had no effect on EGF-stimulated phosphorylation of ERK1 or ERK2 (Fig. 3B), the MAP kinases directly upstream of RSK2. This result further highlights the selectivity of fmk, as the signaling pathway leading to ERK activation involves at least three protein kinases (EGFR, Raf, and MEK), two of which (EGFR and Raf) have threonine gatekeepers, as well as potentially reactive cysteines, in their ATP binding pockets.

We next tested whether inhibition of the CTD by fmk could block signaling downstream of RSK2. In cells transfected with WT RSK2, treatment with EGF induced phosphorylation of histone H3 at Ser¹⁰, which was completely blocked by fmk (Fig. 3C). By contrast, H3 phosphorylation was unaffected by up to 10 μ M fmk in cells expressing the RSK2 gatekeeper mutant, T493M. Mutation of the cysteine selectivity filter to valine (C436V) also conferred complete resistance to fmk (fig. S1). Similar to RSK family kinases, the mitogen- and stress-activated kinases, MSK1 and MSK2, have two kinase domains. The CTD of MSK1 has a cysteine analogous to Cys⁴³⁶ of RSK2 (Fig. 1A), but unlike RSK2, MSK1 has a methionine gatekeeper. Fmk had no effect on H3 phosphorylation mediated by WT MSK1 (Fig. 3D). By contrast, an MSK1 mutant with a threonine gatekeeper was potently inhibited. Thus, despite having only ~40% sequence identity to RSK2, MSK1 became equally sensitive to fmk once the second selectivity filter was introduced. Fmk had no effect on phorbol ester–stimulated H3 phosphorylation in nontransfected fibroblasts (fig. S2), consistent with a dominant role for endogenous MSK1 and MSK2 in this pathway (20).

Pyrrolopyrimidines inhibit Src family kinases such as Fyn (21), which raises the possibility that they might be susceptible to reversible inhibition by cmk or fmk. WT Fyn was weakly inhibited by both compounds, with IC₅₀ values of ~4 μ M (compared with an IC₅₀ value of 15 nM for fmk against RSK2). By contrast, cmk and fmk potently inhibited a Fyn mutant in which Val²⁸⁵ was replaced with Cys (IC₅₀ values of 1 nM and 100 nM, respectively). Similarly, at concentrations that completely inhibited RSK2 in cells, neither cmk nor fmk reversed the cellular phenotypes induced by v-Src (with a Thr in the gatekeeper position). By contrast, cmk (and less potently, fmk) promoted morphological reversion and reduced global tyrosine phosphorylation in cells expressing a v-Src mutant in which Val²⁸¹ was replaced with Cys (fig. S3).

In this study, we have rationally designed halomethylketone-substituted inhibitors whose molecular recognition by protein kinases requires the simultaneous presence of two selectivity filters: a cysteine following the glycine-rich loop and a threonine in the gatekeeper position. We estimate that ~20% of human kinases have a solvent-exposed cysteine in the ATP pocket. Because of the structural conservation of the pocket, it should be possible to predict the orientation of these cysteines. In addition, there are many

reversible kinase inhibitors whose binding modes have been characterized by x-ray crystallography. The integration of both types of information should allow the design of scaffolds that exploit selectivity filters other than the gatekeeper, as well as the appropriate sites for attaching electrophilic substituents.

Supplementary Material

Refer to Web version on PubMed Central for supplementary material.

Acknowledgments

This work was supported by the Searle Scholars Foundation (J.T.), the NIH (K.M.S.), and the ARCS Foundation (M.S.C.). We thank Y. Feng, T. Alber, K. Shah, T. Sturgill, C. Bjorbaek, M. Frodin, and M. Cobb for reagents and S. Arriola for technical assistance. We thank W. Lim, H. Luecke, D. Morgan, B. Shoichet, H. Madhani, and E. O'Shea for advice on the manuscript and members of the Taunton and Shokat laboratories for many helpful discussions. Molecular interaction data have been deposited in the Bimolecular Interaction Network Database (BIND) with accession code 216037.

References and Notes

1. Manning G, Whyte DB, Martinez R, Hunter T, Sudarsanam S. *Science*. 2002; 298:1912. [PubMed: 12471243]
2. Druker BJ, et al. *Nat Med*. 1996; 2:561. [PubMed: 8616716]
3. Barker AJ, et al. *Bioorg Med Chem Lett*. 2001; 11:1911. [PubMed: 11459659]
4. Liu Y, et al. *Chem Biol*. 1999; 6:671. [PubMed: 10467133]
5. Schindler T, et al. *Mol Cell*. 1999; 3:639. [PubMed: 10360180]
6. Zhu X, et al. *Structure Fold Des*. 1999; 7:651. [PubMed: 10404594]
7. Buchdunger E, et al. *J Pharmacol Exp Ther*. 2000; 295:139. [PubMed: 10991971]
8. Fry DW, et al. *Proc Natl Acad Sci U S A*. 1998; 95:12022. [PubMed: 9751783]
9. Buzko O, Shokat KM. *Bioinformatics*. 2002; 18:1274. [PubMed: 12217924]
10. Tsigelny I, et al. *Biopolymers*. 1999; 50:513. [PubMed: 10479734]
11. Sturgill TW, Ray LB, Erikson E, Maller JL. *Nature*. 1988; 334:715. [PubMed: 2842685]
12. Frodin M, Gammeltoft S. *Mol Cell Endocrinol*. 1999; 151:65. [PubMed: 10411321]
13. Hanauer A, Young ID. *J Med Genet*. 2002; 39:705. [PubMed: 12362025]
14. Chrestensen CA, Sturgill TW. *J Biol Chem*. 2002; 277:27733. [PubMed: 12016217]
15. Cohen MS, Taunton J. unpublished data.
16. Canagarajah BJ, Khokhlatchev A, Cobb MH, Goldsmith EJ. *Cell*. 1997; 90:859. [PubMed: 9298898]
17. Vik TA, Ryder JW. *Biochem Biophys Res Commun*. 1997; 235:398. [PubMed: 9199205]
18. Dalby KN, Morrice N, Caudwell FB, Avruch J, Cohen P. *J Biol Chem*. 1998; 273:1496. [PubMed: 9430688]
19. Frodin M, Jensen CJ, Merienne K, Gammeltoft S. *EMBO J*. 2000; 19:2924. [PubMed: 10856237]
20. Soloaga A, et al. *EMBO J*. 2003; 22:2788. [PubMed: 12773393]
21. Burchat AF, et al. *Bioorg Med Chem Lett*. 2000; 10:2171. [PubMed: 11012022]

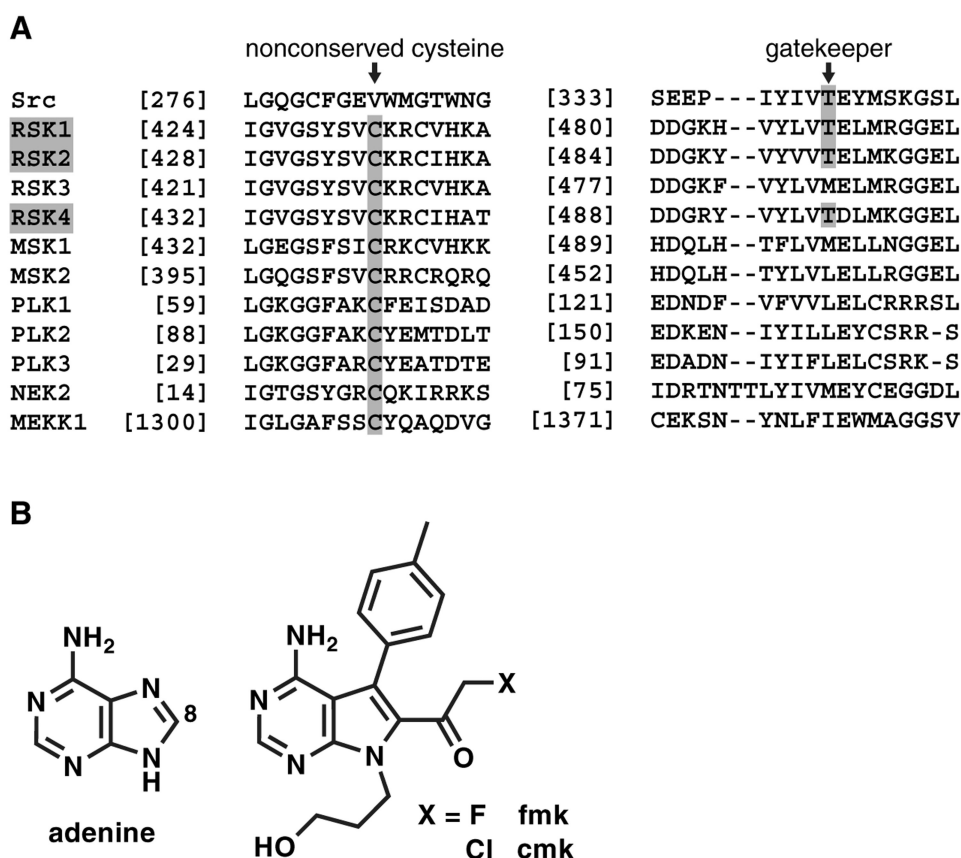
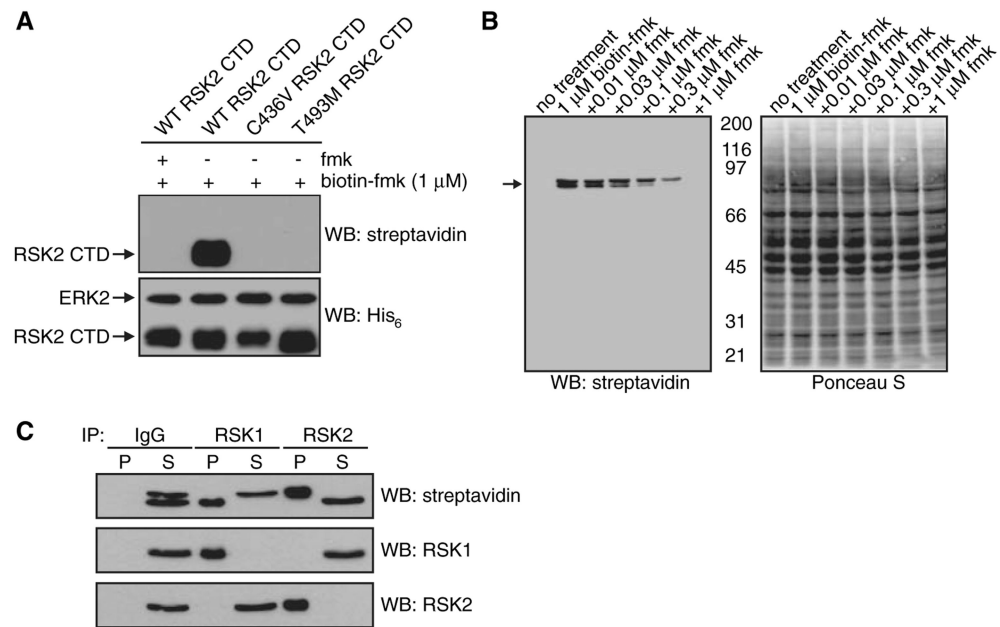
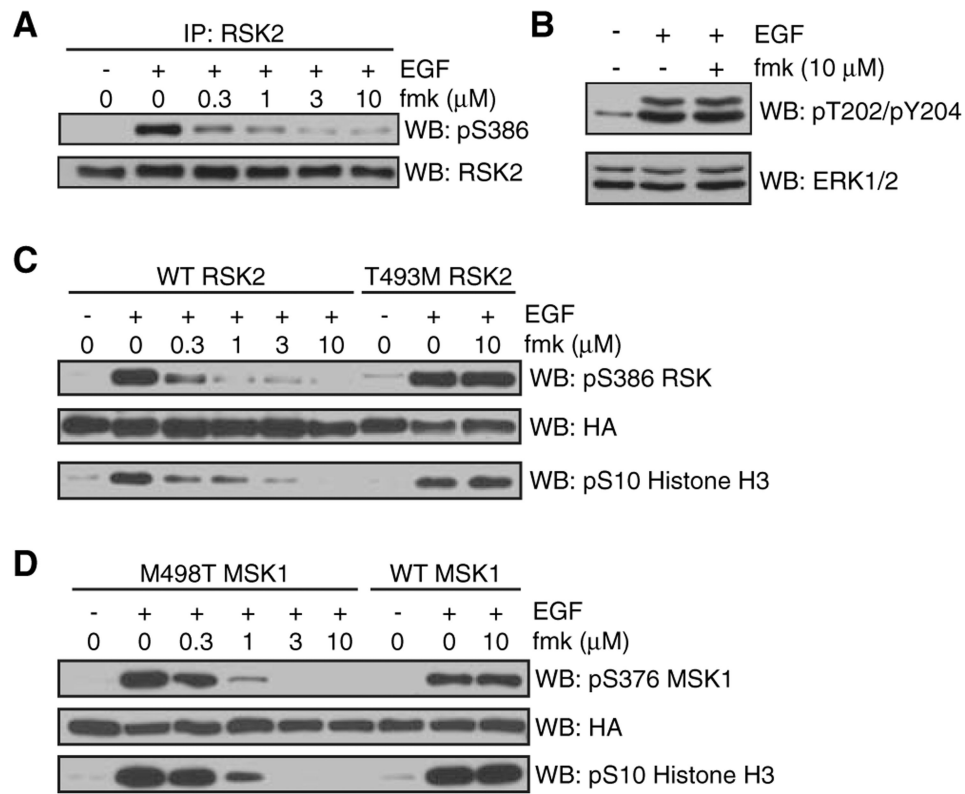


Fig. 1.

Structural bioinformatics guides the design of electrophilic inhibitors of RSK family protein kinases. (A) Sequence alignment of the 11 human kinases with a cysteine selectivity filter at the C-terminal end of the glycine-rich loop. Of these 11, RSK1, RSK2, and RSK4 are the only kinases with a threonine selectivity filter in the gatekeeper position. Src, which has a threonine gatekeeper but lacks the cysteine, is shown for comparison. (B) Chemical structures of adenine and the rationally designed halomethylketone pyrolopyrimidines, cmk and fmk.

**Fig. 2.**

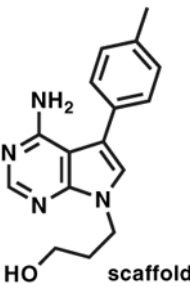
Selective, irreversible targeting of RSK family kinases by fmk. **(A)** Covalent labeling of WT, but not mutant RSK2 by biotin-fmk. RSK2 with a hexahistidine tag (His₆-RSK2) CTDs were treated with 1 μ M biotin-fmk in the presence of His₆-ERK2 for 1 hour. Proteins were resolved by SDS-polyacrylamide gel electrophoresis (SDS-PAGE) and detected by Western blot with streptavidin-HRP or antibodies to His₆. **(B)** Targeting of two ~90-kD proteins in human epithelial cell lysates by biotin-fmk. HEK-293 cell lysates were treated with the indicated concentrations of unlabeled fmk and then with 1 μ M biotin-fmk. Proteins were resolved by SDS-PAGE, transferred to nitrocellulose, and stained with Ponceau S (right). Proteins labeled with biotin-fmk were detected with streptavidin-HRP (left). **(C)** Identification of RSK1 and RSK2 as biotin-fmk targets. HEK-293 lysates were treated with 1 μ M biotin-fmk. Proteins were immunoprecipitated with control IgG, RSK1-specific polyclonal antibodies, or a RSK2-specific monoclonal antibody (Santa Cruz Biotechnology). Immunoprecipitates (P) and supernatants (S) were analyzed by Western blot with streptavidin-HRP and antibodies to RSK1 and RSK2.

**Fig. 3.**

Effect of fmk on EGF-activated RSK2 or MSK1. **(A)** Inhibition of EGF-stimulated RSK2 autophosphorylation by fmk. COS-7 cells were deprived of serum for 20 hours then treated with the indicated concentrations of fmk. Cells were stimulated for 10 min with EGF (1 ng/mL). RSK2 was immunoprecipitated and analyzed by Western blot with antibodies to phospho-Ser³⁸⁶ RSK (Cell Signaling Technology) and total RSK2. **(B)** Failure of fmk to inhibit EGF-stimulated activation of ERK1 and ERK2. Serum-starved COS-7 cells were treated with or without 10 μ M fmk, then stimulated with EGF as in (A). Doubly phosphorylated and total ERK1 and ERK2 were detected by Western blot (both antibodies from Cell Signaling Technology). **(C)** Inhibition of EGF-stimulated H3 phosphorylation in cells expressing WT RSK2, but not T493M RSK2. COS-7 cells were transfected with hemagglutinin (HA)-tagged WT or T493M RSK2. Twenty-four hours after transfection, cells were serum-starved for 3 hours then treated with the indicated concentrations of fmk. Cells were stimulated with EGF (150 ng/mL) for 25 min and subsequently lysed in Laemmli sample buffer. Proteins were resolved by SDS-PAGE and detected by Western blot with antibodies specific for phospho-Ser³⁸⁶ RSK, the HA epitope (Roche), or phospho-Ser¹⁰ H3 (Upstate). **(D)** Inhibition of MSK1 by fmk after mutation of Met⁴⁹⁸ to Thr. COS-7 cells were transfected with HA-tagged WT or M498T MSK1. MSK1 autophosphorylation and H3 phosphorylation were assessed as in (C).

Table 1

Half-maximal inhibitory concentrations (IC_{50} in μM) for fmk and the pyrrolo[2,3-*d*]pyrimidine scaffold against the kinase activities of wild-type (WT) and mutant RSK2 CTDs. RSK2 CTDs were expressed in *E. coli* as His₆-tagged proteins and activated by incubation with bacterially expressed His₆-ERK2 and ATP. Kinase assay conditions: 30-min inhibitor pretreatment, 1 nM RSK2 CTD, 0.1 mM ATP, 0.1 mM “CTD-tide” substrate (14). WT and mutant CTDs had similar kinase activities.

| | WT | C436V | T493M | |
|----------|-------------------|-----------------|---------------|---|
| fmk | 0.015 \pm 0.001 | > 10 | 3.4 \pm 0.3 |  |
| scaffold | 1.2 \pm 0.08 | 0.43 \pm 0.14 | >30 | |